Performance and Stability Improvement of P3HT:PCBM-Based Solar Cells by Thermally Evaporated Chromium Oxide (CrO_x) Interfacial Layer

Mingdong Wang,[†] Qin Tang,[‡] Jin An,[†] Fangyan Xie,[§] Jian Chen,[§] Shizhao Zheng,[⊥] King Young Wong,[⊥] Qian Miao,[‡] and Jianbin Xu*[,†]

Department of Electronic Engineering and Materials Science and Technology Research Center, Department of Chemistry, and Department of Physics, The Chinese University of Hong Kong, Shatin, New Territories, Hong Kong, China, Instrumental Analysis & Research Center, Sun Yat-Sen (Zhongshan) University, Guangzhou, P. R. China 510275

ABSTRACT We report on thermally evaporated chromium oxide (CrO_x) as cathode interfacial layer to improve the efficiency and stability in air for the bulk heterojunction solar cells of poly(3-hexylthiophene) (P3HT) and [6,6]-phenyl C_{61} butyric acid methyl ester (PCBM). Devices with CrO_x interfacial layers show higher power conversion efficiency (PCE) and stability than those without interfacial layer. Devices with CrO_x show improved stability more than 100 times that of devices without interfacial layer or with LiF interfacial layer. We tentatively attributed the CrO_x interfacial layer as an electronic tunneling layer for electron collection and a protective layer of Al assumably by minimizing the organic−Al interfacial areas caused by the evaporation of Al and blocking diffusion of oxygen and water.

KEYWORDS: cathode interfacial layer • bulk heterojunction • solar cells • polythiophene

INTRODUCTION

Polymeric photovoltaic devices promise low-cost production of lightweight, flexible solar cells. Recent progress in polymeric solar cells, has led to power conversion efficiencies (PCEs) of 6−7% (1, 2). In organic/polymeric solar cells, the active layer usually has a thickness of around 100 nm because of its poor electric conductivity. Electrode interface engineering is a key strategy to improve the PCE through optimization of the short circuit current (J_{sc}), open circuit voltage (V_{oc}), fill factor (FF), and the stability (3−7).

It is preferable for the cathode interface to have a low work function contact for efficient electron extraction. Al is the most commonly used electrode material in solar cells, which is generally deposited by thermal evaporation, although this process frequently alters the quality of the metal/organic interface, because the hot metal atoms may react with oxygen species remaining in the vacuum chamber and diffuse into the organic layers. Lögdlund et al. (8) and Antoniadis et al. (9) suggested that the instability of Al electrode is related to the Al−C bond formation, which interrupts the π-conjugated systems. Several cathode interfacial layers such as LiF (10, 11), Ca (12), Ba (13), TiO_x (14, 15), ZnO (16), and Cs_2CO_3 (17) are commonly employed to protect the metal/organic interface in organic devices from thermally evaporated Al. Here, we report on an investigation on thermally evaporated chromium oxide (CrO_x) thin film as a cathode interfacial layer for polymer−fullerene solar cells to improve performance and stability.

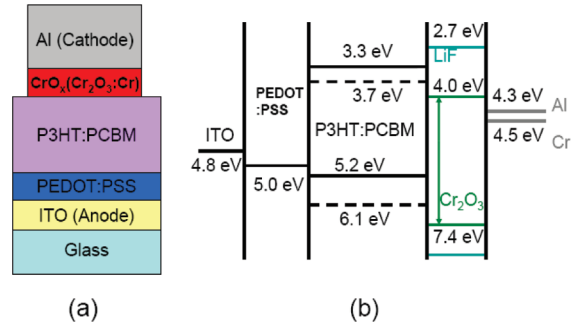

FIGURE 1. (a) Photovoltaic device structure; (b) energy-band diagram composed of different organic layers and interfacial layers.

EXPERIMENTAL SECTION

The device structure is shown in Figure 1 and the fabrication consists of the following steps. Firstly, ITO glass was treated with oxygen plasma for 3 min. Secondly, the PEDOT:PSS was spun cast on ITO glass with a thickness of ca. 40 nm, and then annealed at 145 °C for 10 min in air. A mixed solution composed of P3HT and PCBM in dichlorobenzene was spun cast on the top of PEDOT:PSS layer at a slow speed of 500 rpm for 5 s and a high speed of 1200 rpm for 50 s, with the active layer thickness being 90−110 nm, and then annealed at 120 °C for 10 min in nitrogen atmosphere. The mixed solution had a P3HT:PCBM weight ratio of 1:1 with a concentration of 20 mg/mL. The thin CrO_x layer (ca.5 nm) was deposited by thermal

* Corresponding author. E-mail: jbxu@ee.cuhk.edu.hk.
Received for review June 22, 2010 and accepted August 23, 2010
[†] Department of Electronic Engineering and Materials Science and Technology Research Center, The Chinese University of Hong Kong.
[‡] Department of Chemistry, The Chinese University of Hong Kong.
[§] Sun Yat-sen (Zhongshan) University.
[⊥] Department of Physics, The Chinese University of Hong Kong.
DOI: 10.1021/am100541d

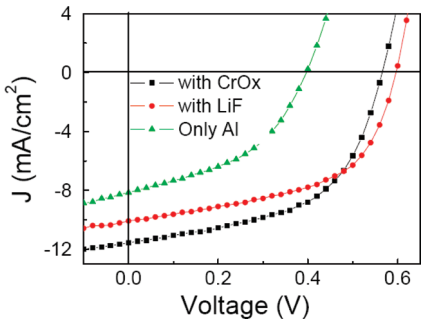

FIGURE 2. $J-V$ characteristics of polymer−fullerene bulk heterojunction devices under illumination with an incident optical intensity of 100 mW/cm^2.

evaporation of chromium metal under a low vacuum (deposited at a base pressure from 1×10^{-4} to 6×10^{-5} mbar). Finally, a 90 nm thick film of Al was thermally evaporated onto the top of the device. The evaporator was BOC Edwards Auto 306. Before evacuation, the chamber was exposed to air for several minutes, without intentional oxygen doping. The active area of device was 2 mm × 1 mm. Electrical measurements were performed by a semiconductor characterization system (Keithley 236) at room temperature in air under the spectral output from solar simulator (Newport) using an AM 1.5G filter with a light power of 100 mW/cm^2. The light intensity was precisely calibrated by a standard solar cell. The devices with LiF as an interfacial layer (ITO/PEDOT:PSS/P3HT:PCBM/LiF/Al, with 1 nm thick LiF), and without the interfacial layer (ITO/PEDOT:PSS/P3HT:PCBM/Al) were also fabricated and tested under the same conditions. For all devices, no external package or encapsulation was applied after device fabrication. The morphologies of the P3HT:PCBM blend thin films, and with LiF or CrO_x over layer were observed by atomic force microscopy (AFM) in the taping mode. The AFM images were taken from actual devices fabricated for measurement of solar performance. The thicknesses of evaporated layers were measured with a thickness monitor (Sigma SQM-160), and also determined by AFM. Mobility is measured by Van der Pauw 4-probe method (18), which is very common to measure the resistivity, mobility, carrier concentration, and Hall effect, especially for semiconductor thin films. There were no requirements for the size and shape of the film, but all four electrodes should be at the edge. A 20 nm thick CrO_x thin film was depsoted on a bare glass substrate, then the glass was cut into the size of 0.5 cm × 0.5 cm, four Al electrodes were deposited at the edge of the CrO_x film. The mobility was obtained from the majority carrier mobility in terms of the calculated sheet resistance and Hall coefficient $\mu = |R_H|/\rho$ (18). BIO RAD Hall System was used to determine the mobility.

RESULTS AND DISCUSSION

Figure 2 shows the current density−voltage ($J-V$) characteristics under illumination. By comparison, it is found that device performance is obviously improved by including the interfacial layer of either LiF or CrO_x. The device with CrO_x (ITO/PEDOT:PSS/P3HT:PCBM/CrO_x/Al) exhibits a PCE as high as 3.5%, with $V_{oc} = 0.56$ V, $J_{sc} = 11.55$ mA/cm^2, and FF = 0.55. In addition to the comparable efficiency improvement, devices with CrO_x show a dramatic improvement of stability, in comparison with those with LiF interfacial layer. The detailed efficiencies, J_{sc}, V_{oc}, and FF are listed in Table 1.

During the deposition of electrode, Al is very easily oxidized, so the deposition pressure is crucial. A layer containing Al_2O_3, an insulator used as dielectric layer in field effect transistor, is often formed during this process, which may lead to a higher contact resistance and lower FF. However, Cr_2O_3, an oxidation product of chromium, is a semiconductor. With 4-probe Hall-effect measurement, thermally evaporated chromium oxide (CrO_x) is determined to be n-type with its mobility of 0.14 cm^2/V · s, which is sufficient to facilitate electron transport in organic solar cells. Moreover, Cr_2O_3 is a very stable semiconductor (19), with its conduction band level of 4.0 eV (20), just between the work function of Al and LUMO of PCBM (shown in Figure 1b), which renders it an efficient electron transport material. The large band gap of 3.4 eV is also capable of blocking the holes and excitons efficiently. In addition, the chromium oxide layer serves as an optical spacer to redistribute light intensity in the active layer, and therefore to increase the short circuit current as previously reported for TiO_x (15). As expected, a low work function material, small LUMO, or small conduction band minimum of interfacial layers in cathode can improve V_{oc}. Cr_2O_3 has a slightly lower conduction band minimum (shown in Figure 1) than that of Al. So inserting CrO_x layer is very likely to result in a higher V_{oc}.

Table 1. Solar Cell Parameters Extracted from Figure 2

sample	efficiency (%)	V_{oc} (V)	J_{sc} (mA/cm^2)	FF
only Al	1.5	0.40	8.55	0.43
with LiF	3.2	0.59	10.08	0.54
with CrO_x	3.5	0.56	11.55	0.55

To collect the compositional information of CrO_x, we performed XPS analysis. XPS spectra are shown in Figure 3. Gaussian−Lorenztzian model is used to analyze the XPS data so as to obtain element ratio and exact positions of peaks. In Figure 3a, the peak at 573.99 eV relates to Cr $2p_{3/2}$ of metallic chromium (21), whereas the peak at 583.37 eV to Cr $2p_{1/2}$ of metallic chromium. And the peak at 576.42 eV relates to Cr $2p_{3/2}$ of chromium oxide (Cr_2O_3) (21−23) while the peak at 586.21 relates to Cr $2p_{1/2}$ of chromium oxide. The O 1s spectrum (Figure 3b) is composed of two peaks. The peak at a binding energy of 530.41 eV corresponds to O in Cr_2O_3 (21−23), and the other peak at binding energy of 531.82 eV is attributed to contamination. The atomic ratio of O to Cr is calculated to be 1.13. The XPS study reveals that the film is oxygen-deficient Cr_2O_3 films with enriched metallic Cr as CrO_x (x being around 1.2). It is well known that Cr metal is easily oxidized. During thermal evaporation under a low vacuum (the base pressure around 1×10^{-4} mbar), some residual oxygen species still existed in the chamber, and hot chromium species were perceived to react with them to form CrO_x. Along with the deposition process, the oxygen species should be decreased. It is plausibly speculated that a perfect CrO_x layer should be Cr_2O_3 in the close proximity of organic−Cr−oxide interface to block holes, while to facilitate electron transport by tunneling. The successive part will be oxygen-deficient with some metallic Cr species for facilitating electron collection. With the control of deposition pressure and rate, oxygen content in CrO_x can be manipulated, resulting in varied optical and electric properties of

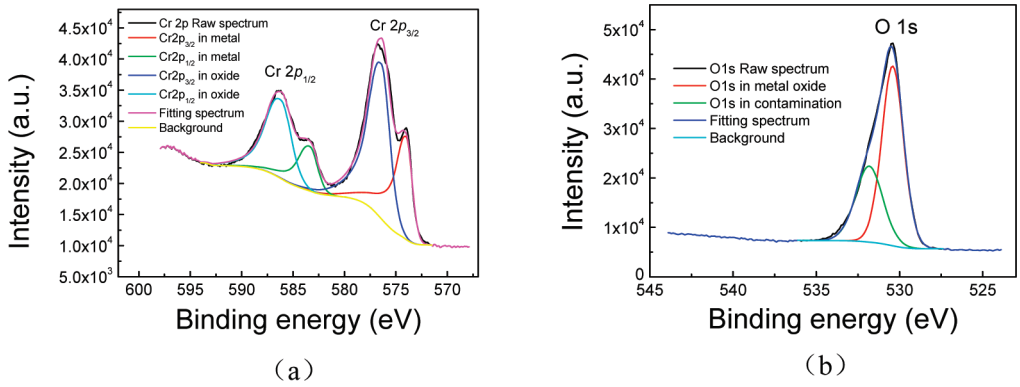

FIGURE 3. Fitted core level XPS spectra of (a) Cr 2*p* peaks, and (b) O 1s peak of the as-deposited CrO_x films.

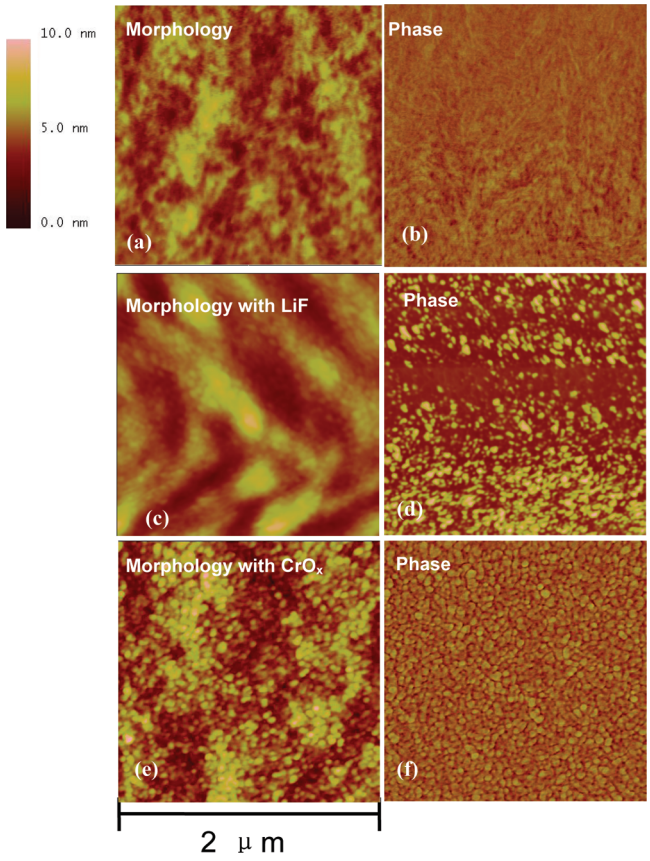

FIGURE 4. AFM images of P3HT:PCBM (ITO\PEDOT:PSS\P3HT:PCBM), (a) morphology and (b) phase; with LiF on P3HT:PCBM (ITO\PEDOT:PSS\P3HT:PCBM\LiF), (c) morphology and (d) phase; with CrO_x (ITO\PEDOT:PSS\P3HT:PCBM\CrO_x), (e) morphology and (f) phase.

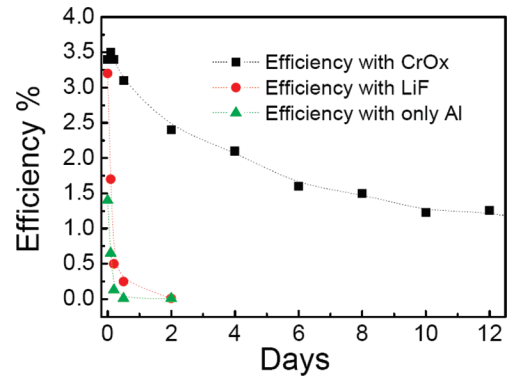

FIGURE 5. Comparison of the power conversion efficiencies as a function of storage time for polymeric solar cells with the interfacial layers of CrO_x, LiF, and without the interfacial layer (only Al). Note that the device characteristics are monitored with increasing storage time for the same devices.

CrO_x. It is naturally expected that the oxygen content will decrease with improvement of the deposition conditions.

Figure 4 shows the AFM topography and phase images of P3HT:PCBM blend thin film before (Figure 4a, b) and after deposition of LiF (Figure 4c, d) and CrO_x (Figure 4e, f). No grains or particles are observed on pristine P3HT:PCBM surface. As shown in AFM images, the surface after deposition of LiF present particles (presumably LiF aggregates), which do not cover the entire surface of the polymeric blend. Both morphology and phase images indicate that the CrO_x layer with an averaged particles size of around 30 nm fully covers the polymer surface. This fully covered CrO_x layer should reduce direct contact between organic materials and Al.

Stability is another important issue for polymeric solar cells (24−26). It is reported that a 30 nm thick TiO_x buffer layer between the active layer and Al cathode and the inverted structure with deposition of Al before spinning active layer obviously improved the stability (15, 27). Here our experiments have shown that the thermally evaporated CrO_x layer indeed improved the lifetime of polymeric solar cells in air. Figure 5 shows the comparison of efficiency versus storage time of the solar cell with CrO_x layer, LiF layer, and without the interfacial layer (only Al). For all devices, no extra package or encapsulation was used. For the devices with LiF interfacial layer and without the interfacial layer stored in ambient air, dramatic decreases in PCE were observed as the storage time increased, and they lost 90% of the initial efficiencies after 5 h, mainly because of the loss of photocurrent. However, for the device with CrO_x interfacial layer, almost no decrease in the first several hours was observed. Nearly 50% of the initial power conversion efficiency still remained after 6 days, and 35% after 12 days.

On the basis of the experimental results above, it can be deduced that the CrO_x layer plays a key role in retarding degradation. During thermal evaporation process, the Al atoms with high kinetic energy flux can diffuse into polymer to form a thick interfacial layer. An approximately 5 nm thick

interfacial layer between the P3HT:PCBM blend and the Al contact was found (28). Theoretically, Lögdlund et al. (8) proposed a direct reaction for the formation of Al−C bond with high reductive power due to Al. An alternative to Al−C was single-electron transfer with the creation of anion radicals on the polymer (8, 29). Both organo-aluminum compounds and anion radicals are highly reactive species that can react with any proton donors present, such as water, or oxygen. Besides, Norrman et al. (30, 29) reported oxygen and water, which can diffuse through the aluminum electrode via microscopic pinholes and metal grains to organic−Al interface and the active layer. It indicates that the thick organic−aluminum interfacial layer between polymer P3HT:PCBM and the Al caused by the evaporated Al is easily oxidized, resulting an barrier for carrier extraction when it is exposed to air. The thermally evaporated and partially oxidized, uniform, and compacted CrO_x buffer layer can improve the device stability because it can effectively avoid or minimize the formation of organic−aluminum interface caused by the evaporation of Al.

In addition, as suggested by the report on TiO_x (31), the CrO_x layer may also function as a robust diffusion barrier against oxygen and water into active layer because of its scavenging effects due to photocatalysis and oxygen deficiency. Although the detailed mechanisms of the stability and degradation issues are rather complicated and certainly not yet fully understood, for the time being, 5−10 nm CrO_x is found to be sufficient to enhance the stability of polymeric solar cells. A thin CrO_x by thermal evaporation under low vacuum conditions will be a useful method for enhancing device lifetime with primary advantages of flexible device concepts, simple fabrication.

In summary, we have found that a CrO_x interfacial layer, which is formed by thermal evaporation of chromium metal under low vacuum conditions, has an ideal energy-band match and electronic properties for electron collection and thus improves the power conversion efficiency of polymer−fullerene BHJ organic solar cells. Moreover, the CrO_x also functions as a protective layer to significantly enhance the device stability assumably by minimizing the organic−Al interfacial areas caused by the evaporation of Al and blocking diffusion of oxygen and water.

Acknowledgment. This work is in part supported by Hong Kong Research Grants Council, particularly, under Grants CUHK02/CRF/08 and CUHK41821/09E. We thank the National Science Foundation of China for the support, particularly, via Grants 60990314 and 60928009. We thank Jun Du and Ning Ke for fruitful discussion and technical support.

REFERENCES AND NOTES

(1) Park, S. H.; Roy, A.; Beaupre, S.; Cho, S.; Coates, N.; Moon, J. S.; Moses, D.; Leclerc, M.; Lee, K.; Heeger, A. J. *Nat. Photonics* **2009**, *3*, 297.
(2) Chen, H. Y.; Hou, J.; Zhang, S.; Liang, Y.; Yang, G.; Yang, Y.; Yu, L.; Wu, Y.; Li, G. *Nat. Photonics* **2009**, *3*, 649.
(3) Cai, W.; Gong, X.; Cao, Y. *Sol. Energy Mater. Sol. Cells* **2010**, *94*, 114–127.
(4) Xue, J.; Rand, B. P.; Uchida, S.; Forrest., S. R. *J. Appl. Phys.* **2005**, *98*, 124903.
(5) Wei, H.Y.; Huang, J. H.; Ho, K. C.; Chu, C. W. *ACS Appl. Mater. Interfaces* **2010**, *2*, 1281–1285.
(6) Kuwabara, T.; Kawahara, Y.; Yamaguchi, T.; Takahashi, K. *ACS Appl. Mater. Interfaces* **2009**, *1*, 2107–2110.
(7) Tromholt, T.; Gevorgyan, S. A.; Jørgensen, M.; Krebs, Frederik, C.; Sylvester-Hvid, Kristian, O. *ACS Appl. Mater. Interfaces,* **2009**, *1*, 2768–277.
(8) Lögdlund, M.; Bredas, J. L. *J. Chem. Phys.* **1994**, *101*, 4357.
(9) Antoniadis, H.; Hsieh, B. R.; Abkowitz, M. A.; Jenekhe, S. A.; Stolka, M. *Synth. Met.* **1994**, *62*, 265.
(10) Shaheen, S. E.; Jabbour, G. E.; Morrell, M. M.; Kawabe, Y.; Kippelen, B.; Peyghambarian, N.; Nabor, M. F.; Schlaf, R.; Mash, E. A.; Armstrong, N. R. *J. Appl. Phys.* **1998**, *84*, 2324.
(11) Hung, L. S.; Zhang, R. Q.; He, P.; Mason, M. G. *J. Phys. D: Appl. Phys.* **2002**, *35*, 103.
(12) Bharathan, J. M.; Yang, Y. *J. Appl. Phys.* **1998**, *84*, 3207.
(13) Reese, M. O.; White, M. S.; Rumbles, G.; Ginley, D. S.; Shaheen, S. E. *Appl. Phys. Lett.* **2008**, *92*, 053307.
(14) Yoon, S. J.; Park, J. H.; Lee, H. K.; Park, O. O. *Appl. Phys. Lett.* **2008**, *92*, 143504.
(15) Kim, J. Y.; Kim, S. H.; Lee, H. H.; Lee, K.; Ma, W.; Gong, X.; Heeger, A. J. *Adv. Mater.* **2006**, *18*, 572.
(16) Kyaw, A. K.; Sun, X. W.; Jiang, C. Y.; Lo, G. Q.; Zhao, D. W.; Kwong, D. L. *Appl. Phys. Lett.* **2008**, *93*, 221107.
(17) Chen, F. C.; Wu, J. L.; Yang, S. S.; Hsieh, K.-H.; Chen, W. C. *J. Appl. Phys.* **2008**, *103*, 103721.
(18) Van der Pauw, L. J. *Philips Tech. Rev.* **1958**, *59*, 220–224.
(19) Pokhrel, S.; Simion, C. E.; Quemenera, V.; Barsan, N.; Weimar, U. *Sens. Actuators, B* **2008**, *133*, 78.
(20) Xu, Y.; Schoonen, M. A. A. *Am. Mineral.* **2000**, *85*, 543–556.
(21) Weaver, J. F.; Hagelin-Weaver, H. A. E.; Hoflund, G. B.; Salaita, G. N. *Appl. Surf. Sci.* **2006**, *252*, 7895–7903.
(22) Barshilia, H. C.; Selvakumar, N.; Rajam, K. S.; Biswas, A. *J. Appl. Phys.* **2008**, *103*, 023507.
(23) Cheng, R.; Xu, B.; Borca, C. N.; Sokolov, A.; Yang, C.-S.; Yuan, L.; Liou, S.-H.; Doudin, B.; Dowben, P. A. *Appl. Phys. Lett.* **2001**, *79*, 3122–3124.
(24) Medford, A. J.; Lilliedal, M. R.; Jørgensen, M.; Aarø, D.; Pakalski, H.; Fyenbo, J.; Krebs, F. C. *Opt. Express.* **2010**, *103*, A272–A285.
(25) Krebs, F. C.; Tromholt, T.; Jørgensen, M. *Nanoscale* **2010**, *2*, 873–886.
(26) Krebs, F. C.; Nielsen, T. D.; Fyenbo, J.; Wadstrøm, M.; Pedersen, M. S. *Energy Environ. Sci.* **2010**, *3*, 512–525.
(27) Zimmermann, B.; Wurfel, U.; Niggemann, M. *Sol. Energy Mater. Sol. Cells* **2009**, *93*, 491.
(28) Nam, C. Y.; Su, D.; Black, C. T. *Adv. Funct. Mater.* **2009**, *19*, 1.
(29) Jørgensen, M.; Norrman, K.; Krebs, F. C. *Sol. Energy Mater. Sol. Cells* **2008**, *92*, 686.
(30) Norrman, K.; Krebs, F. C. *Sol. Energy Mater. Sol. Cells* **2006**, *90*, 213.
(31) Lee, K.; Kim Jin, Y.; Park, S. H.; Kim, S. H.; Cho, S.; Heeger, A. J. *Adv. Mater.* **2007**, *19*, 2445.

AM100541D